IIETA International Information and Engineering Technology Association
Advancing the World of Information and Engineering

Journal Européen des Systèmes Automatisés
Vol. 59, No. 1, January, 2026, pp. 61-67
Journal homepage: http://iieta.org/journals/jesa

Optimization of GMAW Parameters for Enhanced Weld Joint Strength in Offshore Wind Turbine Structures Using A572 Grade 50 Steel

Minh Hung Vu[1], Quoc Manh Nguyen[2], Tien Huy Nguyen[1], Minh Hue Pham Thi[3], Van Thinh Nguyen[2], The-Vinh Do[4*]

[1] Faculty of Fundamental Sciences, Petro Vietnam University, Ho Chi Minh City 70000, Vietnam
[2] Faculty of Mechanical Engineering, Hung Yen University of Technology and Education, Hung Yen 17000, Vietnam
[3] School of Mechanical and Automobile, Hanoi Industry University, Hanoi City 10000, Vietnam
[4] Faculty of Mechanical Engineering, Thai Nguyen University of Technology, Thai Nguyen 24000, Vietnam

Corresponding Author Email: thevinh8880@tnut.edu.vn

https://doi.org/10.18280/jesa.590107

Received: 13 November 2025
Revised: 20 January 2026
Accepted: 29 January 2026
Available online: 31 January 2026

Keywords:
Gas Metal Arc Welding, A572 Grade 50 steel, weld joint strength, impact toughness, parameter optimization, Analysis of Variance, offshore wind turbine structures

ABSTRACT

This study investigates the optimization of Gas Metal Arc Welding (GMAW) parameters to enhance the mechanical properties of welded joints in A572 Grade 50 steel, a material widely employed in offshore wind turbine structures. The effects of three key welding parameters—welding current (I), arc voltage (U), and welding travel speed (V)—on tensile strength and impact toughness were examined. Nine welding trials were designed using a Taguchi L9 orthogonal array, and mechanical performance was evaluated through tensile and Charpy impact tests. Analysis of Variance (ANOVA) and signal-to-noise (S/N) ratio analyses were employed to identify the most influential parameters and determine optimal welding conditions. The results indicate that welding current has the most significant effect on both tensile strength and impact toughness, followed by voltage, while welding speed shows a comparatively minor influence. The optimal parameter combination was identified as 125 A current, 20 V voltage, and 3.5 mm/s welding speed. High coefficients of determination were obtained (R^2 = 98.97% for tensile strength and 95.94% for impact toughness), confirming the reliability of the statistical analysis. These findings provide practical guidance for improving weld joint performance in offshore wind turbine tower fabrication using GMAW.

1. INTRODUCTION

The global shift towards renewable energy has accelerated the deployment of offshore wind energy systems, where structural integrity is critical [1]. Offshore wind turbine towers, such as monopiles and jackets, face harsh marine environments, dynamic loading, and fatigue [2-4]. The reliability of welded joints in these structures is essential for safety and durability [5-7].

ASTM A572 Grade 50 steel is widely used in offshore wind turbine structures due to its high strength-to-weight ratio and weldability [8, 9]. Gas Metal Arc Welding (GMAW) is commonly employed for its high deposition rates and automation potential [10-12]. However, GMAW process parameters significantly influence weld quality, particularly tensile strength and impact toughness, which are vital for offshore conditions [13].

Research has explored how welding parameters affect A572 Grade 50 steel welds. For example, a study investigated the behavior of the heat-affected zone (HAZ) and weld bead under various welding conditions, emphasizing parameter optimization for mechanical properties [14, 15]. Another study examined the effect of heat input on welded joint properties of A572 Grade 50 steel using GMAW with 90% Ar–10% CO_2 shielding gas and spray metal transfer, highlighting heat input's role in weld quality [16]. Additionally, studies on high-strength low-alloy (HSLA) steels have shown that welding current and voltage affect tensile strength and weld geometry, supporting the need for precise control [17].

Despite these efforts, a comprehensive statistical analysis of GMAW parameters for A572 Grade 50 steel in offshore wind applications is lacking. This study investigates the effects of welding current, voltage, and travel speed on the mechanical properties of GMAW-welded A572 Grade 50 steel. Using experimental trials, Analysis of Variance (ANOVA), and regression modeling, it aims to optimize parameters for enhanced tensile strength and impact toughness, contributing to quality assurance in offshore wind turbine fabrication.

2. EXPERIMENTAL SETUP

2.1 Materials

ASTM A572 Grade 50 carbon steel plates (10 mm thick), used in Vietnam for wind turbine towers, were selected as the base material. Table 1 lists its chemical composition. The filler was BÖHLER Q 71.1 RC flux-cored wire (1.2 mm diameter),

manufactured by BÖHLER welding. Weld metal properties are listed in Table 2.

Table 1. Chemical composition of A572 Grade 50 steel (wt%)

C	Si	Mn	P	S	Nb	V
0.23	0.40	1.35	0.04	0.05	0.005–0.05	0.01–0.15

Table 2. Weld metal properties (BÖHLER Q 71.1 RC)

Yield Strength (MPa)	Tensile Strength (MPa)	Impact Toughness (J, -20°C)
≥ 470	550–650	≥ 47

2.2 Welding equipment

Welding was performed using an HK MIG 350 MIG/MAG machine in constant voltage mode. For microstructure analysis, an Axiovert 5 inverted optical microscope was used.

2.3 Specimen preparation

Plates (200 mm × 150 mm × 10 mm) were plasma-cut with a V-groove (60° angle), cooled naturally, and ground to remove oxides. Pairs were tack-welded with a 2.5 mm root gap, and a ceramic backing strip (6 mm groove) supported the root pass.

2.4 Welding procedure

Welding was carried out in the flat position using a three-pass technique to completely fill the V-groove. The experiments were designed according to a Taguchi L9 (3^3) orthogonal array, in which welding current, arc voltage, and welding travel speed were varied at three levels, resulting in nine experimental runs (Table 3).

Table 3. Welding parameters

Parameter	Low	Medium	High
Current (A)	120	125	130
Voltage (V)	18	20	22
Travel Speed (mm/s)	3	3.5	4.0

The selected parameter levels were carefully determined based on preliminary trials to ensure stable arc conditions and adequate weld penetration, which are essential for achieving high-quality welds. Throughout all experiments, the shielding gas flow rate was kept constant at 10 L/min to maintain a stable welding environment, and the inter-pass temperature was consistently maintained below 200°C to avoid any deterioration of the weld metal and HAZ toughness.

2.5 Testing

Tensile specimens (ASTM E8/E8M, 50 mm gauge) and Charpy V-notch specimens (ASTM E23, weld metal notch) were tested. Tensile tests (100 kN machine, 2 mm/min) measured yield and tensile strength. Impact tests at -3°C measured absorbed energy. For each experimental condition, three specimens were tested, and the reported values represent the average of the three measurements.

3. RESULT AND DISCUSSIONS

Table 4 presents the experimental results of butt welding A572 Grade 50 steel using the GMAW process. The experiments were designed based on the Taguchi L9 orthogonal array to optimize key welding parameters. Each value reported in Table 4 corresponds to the average result obtained from three replicate tests. The input parameters include welding current (I), voltage (U), and welding speed (V). The output responses measured are: tensile strength (Fk), and impact toughness (Fv).

Among the nine welding trials, experiment No. 5, with the parameter combination of I = 125 A, U = 20 V, and V = 3.5 mm/s, yielded the best results, achieving the highest tensile strength of 480 MPa and the highest impact toughness of 185J.

Table 4. The experimental results

No.	I (A)	U (V)	V (mm/s)	Fk (MPa)	Fv (J)
1	120	18	3.0	460	150
2	120	20	3.5	470	160
3	120	22	4.0	465	155
4	125	18	3.5	472	165
5	125	20	3.5	480	185
6	125	22	3.0	470	170
7	130	18	4.0	468	160
8	130	20	3.0	475	175
9	130	22	3.5	469	168

3.1 Effects of welding parameters on tensile strength

Figure 1 illustrates the main effects plot for the signal-to-noise (S/N) ratio corresponding to the tensile strength of the welds. This plot provides insights into how each welding parameter—current (I), voltage (U), and welding speed (V)—influences the tensile strength under the Taguchi design framework.

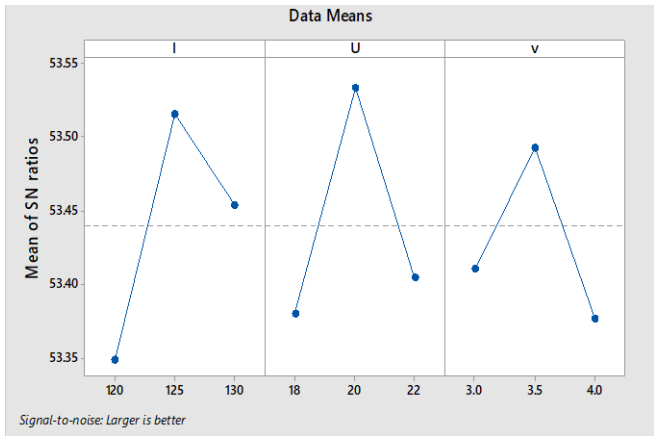

Figure 1. The main effects plot for signal-to-noise (S/N) ratio corresponding to the tensile strength

Welding current (I) shows the most significant effect. The S/N ratio increases markedly as the current rises from 120 A to 125 A, indicating improved tensile strength. However, a slight decline is observed when the current increases further to 130A, suggesting that 125 A is the optimal current level. Excessive current can cause overheating, leading to grain coarsening in the HAZ, which reduces tensile strength. Welding voltage (U) has a moderate influence. The tensile strength improves when the voltage increases from 18 V to 20

V, but declines at 22 V. A voltage of 20 V provides a stable arc and adequate penetration, enhancing joint quality. Higher voltages tend to widen the arc, reducing penetration and weakening the weld. Welding speed (V) has the least effect. As the speed increases from 3.0 mm/s to 4.0 mm/s, the S/N ratio—and thus tensile strength—gradually decreases. Lower welding speeds (around 3.0 – 3.5 mm/s) allow more heat input and better fusion, which are beneficial for tensile strength. At higher speeds, reduced heat input can result in shallow penetration and poor bonding. These trends confirm that welding current is the most influential parameter for tensile strength optimization in GMAW of A572 Grade 50 steel. These observations are consistent with the results presented in Table 5, which summarizes the average tensile strength responses at each factor level.

Table 5. The average tensile strength responses

Level	I	U	V
1	465.0	466.7	468.3
2	474.0	475.0	472.8
3	470.7	468.0	466.5
Delta	9	8.3	6.3
Rank	1	2	3

The ranking in the table confirms that welding current (I) has the highest impact (Delta = 9), followed by voltage (U) (Delta = 8.3), and welding speed (V) (Delta = 6.3), further validating that current is the most critical parameter influencing weld joint strength. To quantitatively evaluate the influence of the welding parameters on tensile strength, an ANOVA was conducted. ANOVA was performed using the experimental response data to evaluate the contribution of each welding parameter based on the variability of tensile strength around its mean value. The corresponding ANOVA results are summarized in Table 6.

As shown in Table 6, among the three input parameters, welding current has the most significant effect, with the highest F-value (43.41) and a P-value of 0.023, indicating strong statistical significance. Welding voltage also shows a significant influence (F = 39.40, P = 0.025). In contrast, welding speed has minimal impact, with a P-value of 0.185, meaning it is not statistically significant. The small error term confirms high experimental precision. Furthermore, the regression model demonstrates excellent predictive capability, with a coefficient of determination R^2 = 98.97%, indicating that nearly all variations in tensile strength can be explained by the selected welding parameters. Overall, current is the dominant factor, followed by voltage, while speed has a negligible effect.

Table 6. Analysis of Variance for tensile strength

Source	DF	Adj-SS	Adj-MS	F-Value	P-Value
I	2	115.767	57.883	43.41	0.023
U	2	105.067	52.533	39.40	0.025
V	2	11.778	5.889	4.42	0.185
Error	2	2.667	1.333	-	-
Total	8	258.889	-	-	-
R^2 = 98.97%					

3.2 Effects of welding parameters on impact toughness

Figure 2 presents the main effects plot for the (S/N) ratio of impact toughness, illustrating the influence of three welding parameters—current (I), voltage (U), and welding speed (V)—on the ability of the weld joint to absorb impact energy.

Welding current (I) has the strongest effect. The S/N ratio significantly increases from 120 A to 125 A, indicating improved impact toughness, then slightly decreases at 130 A. This suggests that 125 A is the optimal current level for maximizing energy absorption. Excessive current can enlarge the HAZ and promote grain growth, leading to reduced toughness.

Welding voltage (U) also shows a notable influence. The S/N ratio increases from 18 V to 20 V, then drops at 22 V. A voltage of 20 V appears optimal for maintaining arc stability and minimizing defects. Higher voltages may overheat the weld pool and degrade the microstructure, reducing toughness.

Welding speed (V) exhibits the least effect. The S/N ratio slightly decreases as speed increases from 3.0 mm/s to 4.0 mm/s, suggesting that lower speeds help retain better impact resistance. Faster welding reduces heat input and cooling time, which can lead to the formation of brittle phases.

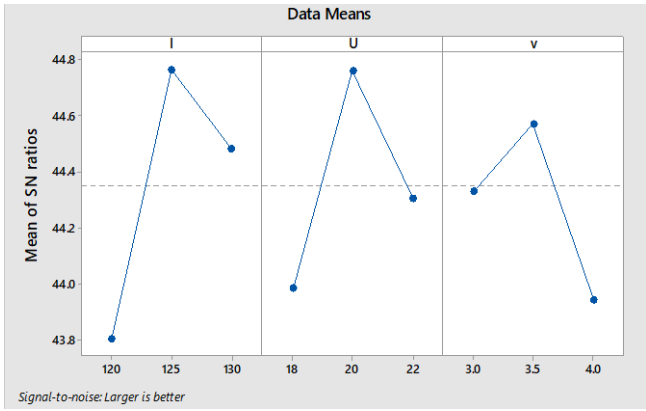

Figure 2. Main effects plot for S/N ratio of impact toughness

These trends align with the results shown in Table 7, where the average impact toughness values and ranking confirm that current has the strongest influence, followed by voltage, and welding speed has the lowest effect.

Table 7. The average impact toughness responses

Level	I	U	V
1	155.0	158.3	165.0
2	173.3	173.3	169.5
3	167.7	164.3	157.5
Delta	18.3	15.0	12.0
Rank	1	2	3

Similarly, ANOVA was applied to assess the statistical significance of welding parameters on impact toughness. The analysis was carried out using the experimental impact toughness data to quantify the contribution of each parameter. The ANOVA results are presented in Table 8.

As shown in Table 8, welding current has the most significant influence, with the highest F-value (12.79) and Adj-SS = 471.067. Although the P-value = 0.073 is slightly above 0.05, it still indicates a considerable effect.

Welding voltage ranks second, but its P-value = 0.115 suggests a weaker and statistically insignificant influence. Welding speed has a negligible effect, with an almost zero F-value (0.01) and P-value = 0.987.

Table 8. ANOVA for impact toughness

Source	DF	Adj-SS	Adj-MS	F-Value	P-Value
I	2	471.067	235.533	12.79	0.073
U	2	284.400	142.200	7.72	0.115
V	2	0.500	0.250	0.01	0.987
Error	2	36.833	18.417	-	-
Total	8	908.000	-	-	-
$R^2 = 95.94\%$					

The regression model shows good predictive power, with $R^2 = 95.94\%$, meaning most of the variation in impact toughness is explained by the welding parameters. Overall, welding current exhibits the strongest influence on the responses, followed by arc voltage, whereas welding speed shows a comparatively minor effect.

It is noted that the identified optimal parameter combination (125 A, 20 V, and 3.5 mm/s) corresponds to the medium levels of the investigated factors. This behavior can be explained by the combined effect of welding current, voltage, and travel speed on the welding heat input. Heat input, which is proportional to the ratio of arc power (I × U) to welding speed, governs the thermal cycle experienced by the weld metal and HAZ.

At lower parameter levels, insufficient heat input may result in inadequate fusion and reduced mechanical performance, whereas excessive heat input at higher levels can promote grain coarsening in the HAZ and degradation of impact toughness. The medium parameter combination provides a balanced heat input condition, leading to improved tensile strength and impact toughness by ensuring adequate penetration while limiting adverse thermal effects.

From an application perspective, the achieved impact toughness of 185 J at −3°C indicates a high level of fracture resistance for the welded joint. According to commonly referenced offshore structural guidelines, such as DNV and ISO standards for welded steel structures, absorbed impact energy values in the range of 27–47 J at sub-zero temperatures are typically considered acceptable for structural integrity. Although the present study does not aim to certify compliance with specific standards, the obtained impact toughness significantly exceeds these indicative requirements, demonstrating the suitability of the optimized GMAW parameters for offshore wind turbine tower applications.

3.3 Characterization of weld joint properties under optimized Gas Metal Arc Welding parameters

To comprehensively evaluate the quality of the weld joint produced under optimal GMAW parameters, a detailed analysis of its macrostructure, microstructure, and microhardness was conducted. The optimal welding conditions, determined as welding current (I) of 125 A, voltage (U) of 20 V, and welding speed (V) of 3.5 mm/s, were applied to fabricate butt welds on A572 Grade 50 steel plates. These parameters yielded superior mechanical properties, with a tensile strength of 480 MPa and impact toughness of 185 J, as established in the experimental results. This section investigates the structural characteristics of the weld joint to elucidate the relationship between the optimized parameters and the resulting weld integrity, focusing on the macrostructure, microstructural variations across different weld zones, and microhardness distribution.

3.3.1 Macrostructure of the weld joint

Figure 3 illustrates the macrostructure of the butt weld joint in A572 Grade 50 steel. After polishing and etching, the weld cross-section revealed four distinct regions, labeled 1 to 4, corresponding to the areas analyzed for microstructural characteristics. These regions include the base metal (region 1), the HAZ (region 2), the weld metal (region 3), and the fusion boundary between the weld metal and HAZ (region 4). As the weld joint involves identical base materials, the thermal effects and resultant structural properties are symmetrical on both sides of the weld. Consequently, analyzing one side of the joint is sufficient to characterize the weld's overall behavior, ensuring an efficient yet comprehensive evaluation of the macrostructure.

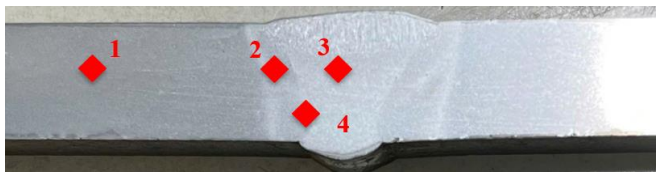

Figure 3. Macrostructure of the butt-welded joint in A572 Grade 50 steel under optimized GMAW parameters, showing the base metal (1), heat-affected zone (2), weld metal (3), and fusion boundary (4)

3.3.2 Microstructure and microhardness of the weld joint

The microstructural observations presented here are intended to provide qualitative insight into the weld zones under optimized GMAW conditions. The microstructure of the weld joint produced under optimal GMAW parameters (welding current: 125 A, voltage: 20 V, welding speed: 3.5 mm/s) was analyzed to elucidate the influence of thermal effects on the weld's structural characteristics. Four regions, identified in the macrostructure (Figure 3), were examined: base metal (region 1), heat-affected zone (HAZ, region 2), weld metal (region 3), and fusion boundary (region 4). Additionally, microhardness measurements were conducted across these regions to assess variations in mechanical properties.

Figure 4 depicts the microstructure of the base metal, located in region 1, far from the weld's thermal influence. The A572 Grade 50 steel, a carbon steel, exhibits a characteristic ferrite-pearlite structure, with pearlite appearing as dark phases and ferrite as bright phases.

This microstructure, consistent with the steel's chemical composition (as described in Table 1), remains unaltered due to its distance from the heat source, in agreement with observations reported in previous studies [18, 19].

The microstructure of the HAZ, shown in Figure 5 (region 2), retains the ferrite-pearlite structure typical of A572 Grade 50 steel.

However, thermal exposure during welding results in a denser pearlite distribution and less uniform ferrite arrangement compared to the base metal. This altered microstructure, characterized by increased pearlite content, reflects the significant thermal influence during welding, consistent with microstructural trends reported in the literature [19].

Figure 6 illustrates the microstructure of the weld metal in region 3, directly affected by the welding heat and filler material (BÖHLER Q 71.1 RC flux-cored wire). The ferrite-pearlite structure persists, but the pearlite exhibits varied morphologies, including fibrous forms and isolated, short

pearlite grains scattered across the region. These structural changes, influenced by the filler wire's composition, contribute to enhanced mechanical properties of the weld joint compared to conventional welds.

The microstructure at the fusion boundary, shown in Figure 7 (region 4), displays a distinct transition between the HAZ and weld metal. In the HAZ adjacent to the A572 Grade 50 steel, a dense interweave of pearlite and ferrite is observed.

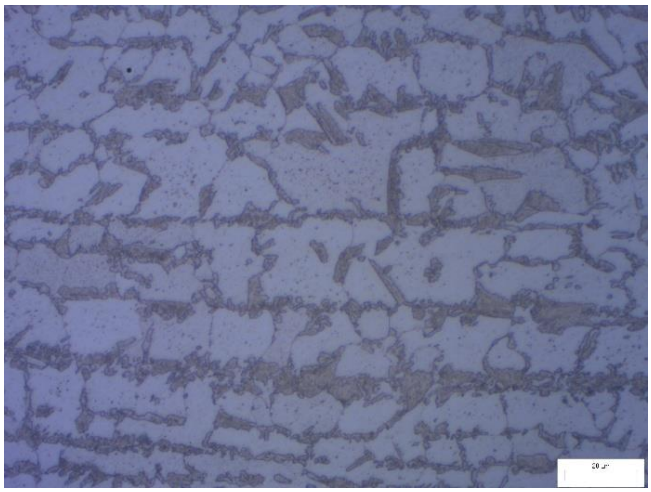

Figure 4. Microstructure of the A572 Grade 50 steel base metal (region 1)

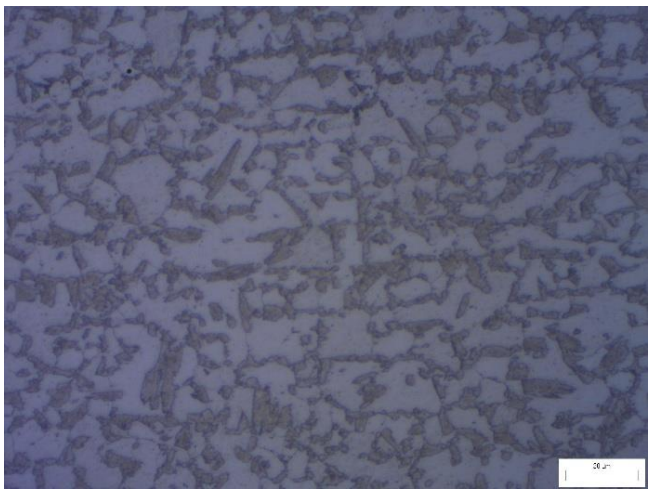

Figure 5. Microstructure of the HAZ (region 2)

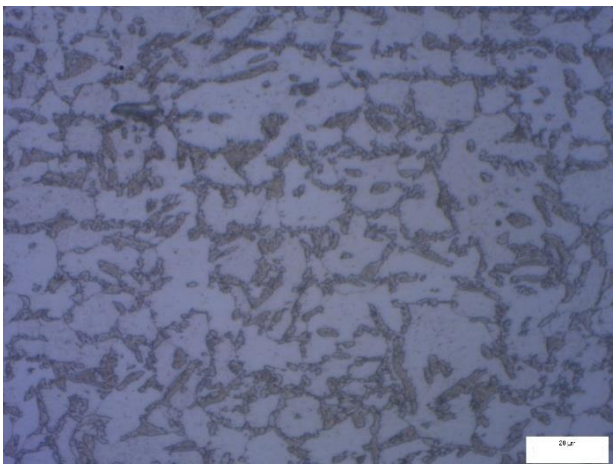

Figure 6. Microstructure of the weld metal (region 3)

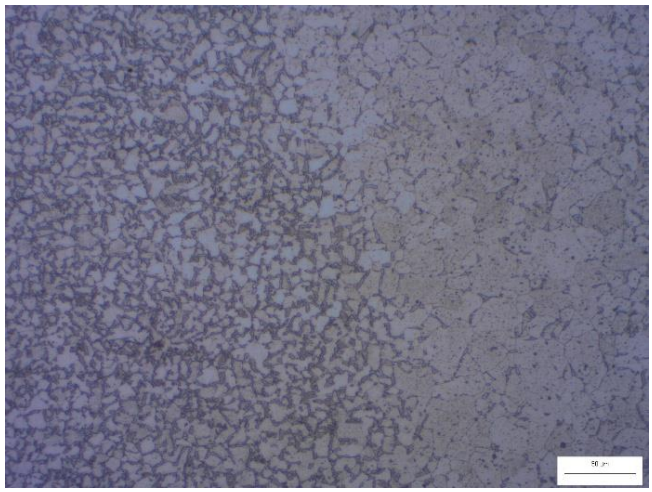

Figure 7. Microstructure of the fusion boundary (region4)

At the boundary, the structure shifts to a ferrite-dominated matrix. This abrupt microstructural change may reduce tensile strength in this region, particularly in low- and medium-carbon steels, as reported in previous studies [20], potentially contributing to fracture during tensile testing.

Microhardness measurements were used to compare relative hardness variations among different weld regions. Table 9 presents the microhardness values measured across the base metal, HAZ, weld metal, and fusion boundary.

Table 9. Microhardness of the A572 Grade 50 steel butt weld joint

Measurement Location	Region				Average
	1	2	3	4	
Microhardness (HV)	157	152	155	165	157.25

Hardness increases from the base metal (157 HV) toward the weld metal (165 HV), with the lowest value recorded in the HAZ (152 HV). The average microhardness is 157.25 HV, with a maximum variation of 13 HV between the HAZ and weld metal. This modest hardness variation indicates good structural uniformity. The lower hardness in the HAZ suggests it as the likely fracture location during tensile testing, corroborating the predicted mechanical behavior under optimal welding parameters.

The weld joint's macrostructure demonstrates clear delineation of the base metal, HAZ, weld metal, and fusion boundary, with no visible defects, ensuring a sound weld profile. The microstructure across these regions exhibits stable ferrite-pearlite phases with controlled thermal-induced variations, supporting consistent mechanical behavior. The microhardness distribution, with minimal variation, further confirms the weld's homogeneity and strength. Collectively, these characteristics—sound macrostructure, balanced microstructure, and uniform microhardness—satisfy the criteria for a high-quality weld, capable of withstanding the demanding conditions of offshore wind turbine structures.

4. CONCLUSION

This study optimized GMAW parameters for A572 Grade 50 steel, achieving a tensile strength of 480 MPa and impact toughness of 185 J at 125 A, 20 V, and 3.5 mm/s. Welding current was identified as the dominant factor, followed by

voltage, while welding speed exhibited a minimal influence, as confirmed by ANOVA and S/N ratio analyses ($R^2 = 98.97\%$ for tensile strength and 95.94% for impact toughness).

The weld joint exhibited a sound macrostructure with clearly defined regions, including the base metal, HAZ, weld metal, and fusion boundary, without observable welding defects. Microstructural observations indicated typical ferrite–pearlite features in the base metal, localized microstructural variations in the HAZ, and characteristic weld metal morphology under the optimized welding conditions. Microhardness values ranged from 152 HV in the HAZ to 165 HV in the weld metal, with an average value of 157.25 HV, reflecting relatively uniform hardness distribution across the joint.

Overall, the combined mechanical performance, macrostructural integrity, and metallurgical observations demonstrate that the optimized GMAW parameters are suitable for producing reliable welded joints for offshore wind turbine tower applications. Future work will focus on fatigue performance evaluation under cyclic loading and validation of the proposed parameters on different joint geometries, in addition to more detailed microstructural and fracture behavior analyses.

ACKNOWLEDGMENT

The authors gratefully acknowledge the support provided by Thai Nguyen University of Technology for conducting this research.

REFERENCES

[1] Weeks, D. (2024). Renewables 2024 Global Status Report: Global Overview.

[2] Bhattacharya, S. (2019). Design of Foundations for Offshore Wind Turbines. John Wiley & Sons.

[3] Wu, X., Hu, Y., Li, Y., Yang, J., Duan, L., Wang, T., Liao, S. (2019). Foundations of offshore wind turbines: A review. Renewable and Sustainable Energy Reviews, 104: 379-393. https://doi.org/10.1016/j.rser.2019.01.012

[4] Arshad, M., O'Kelly, B.C. (2013). Offshore wind-turbine structures: A review. Proceedings of the Institution of Civil Engineers-Energy, 166(4): 139-152. https://doi.org/10.1680/ener.12.00019

[5] Amaechi, C.V., Reda, A., Butler, H.O., Ja'e, I. A., An, C. (2022). Review on fixed and floating offshore structures. Part I: Types of platforms with some applications. Journal of Marine Science and Engineering, 10(8): 1074. https://doi.org/10.3390/jmse10081074

[6] Mehmanparast, A., Adedipe, O., Brennan, F., Chahardehi, A. (2016). Welding sequence effects on residual stress distribution in offshore wind monopile structures. Fracture and Structural Integrity, 10(35): 125-131. https://doi.org/10.3221/IGF-ESIS.35.15

[7] Schaumann, P., Böhm, M., Schürmann, K. (2021). Improvements in the fatigue design of support structures for offshore wind turbines. Steel Construction, 14(2): 74-82. https://doi.org/10.1002/stco.202000060

[8] Guthrie, R.I.L., Jonas, J., ASM, M. H.V. (1990). Properties and Selection: Irons, Steels, and High-Performance Alloys, ASM International. https://doi.org/10.31399/asm.hb.v01.9781627081610

[9] Yin, F., Zhou, H., Wang, Y.Q., Liao, X.W., Yang, L. (2018). Fracture properties of butt weld of A572 Gr. 50 thick steel plates. Engineering Mechanics, 35(6): 42-51.

[10] Weman, K. (2011). Welding Processes Handbook. Elsevier.

[11] Ibrahim, I.A., Mohamat, S.A., Amir, A., Ghalib, A. (2012). The Effect of Gas Metal Arc Welding (GMAW) processes on different welding parameters. Procedia Engineering, 41: 1502-1506. https://doi.org/10.1016/j.proeng.2012.07.342

[12] Norrish, J. (2017). Recent gas metal arc welding (GMAW) process developments: The implications related to international fabrication standards. Welding in the World, 61(4): 755-767. https://doi.org/10.1007/s40194-017-0463-8

[13] Kah, P., Suoranta, R., Martikainen, J. (2013). Advanced gas metal arc welding processes. The International Journal of Advanced Manufacturing Technology, 67(1): 655-674. 10.1007/s00170-012-4513-5.

[14] Deo, M., Tewari, S.P., Mahobia, G.S. (2020). Behaviour of HAZ and weld bead under different welding condition for A572 GR 50 steel. International Journal of Advanced Research in Engineering and Technology, 11(6).

[15] Adak, D.K., Mukherjee, M., Pal, T.K. (2015). Development of a direct correlation of bead geometry, grain size and HAZ width with the GMAW process parameters on bead-on-plate welds of mild steel. Transactions of the Indian Institute of Metals, 68(5): 839-849. https://doi.org/10.1007/s12666-015-0518-8

[16] Díaz Ávila, Á.M., Herrera De Oro, E.D.J., Medellín Pérez, E.C., Niebles Núñez, E.E., Unfried-Silgado, J. (2023). Evaluation of the effect of heat input on welded joint properties of ASTM A572 grade 50 steel using the GMAW process with 90Ar-10CO 2 shielding gas and spray metal transfer. Soldagem & Inspeção, 28: e2805. https://doi.org/10.1590/0104-9224/SI28.05

[17] Rafique, M.MA. (2024). Corrosion and microstructure evolution of ultrasonic (UaFSW), induction (i-FSW) and laser heating assisted macro and micro (μFSW) dissimilar friction stir welding and friction stir spot welding (FSSW)(surface and underwater deep sea) steels and Aluminum alloys. Available at SSRN 4741347.

[18] Güral, A., Bostan, B., Özdemir, A.T. (2007). Heat treatment in two phase region and its effect on microstructure and mechanical strength after welding of a low carbon steel. Materials & Design, 28(3): 897-903. https://doi.org/10.1016/j.matdes.2005.10.005

[19] Khorrami, M.S., Mostafaei, M.A., Pouraliakbar, H., Kokabi, A.H. (2014). Study on microstructure and mechanical characteristics of low-carbon steel and ferritic stainless steel joints. Materials Science and Engineering: A, 608: 35-45. https://doi.org/10.1016/j.msea.2014.04.065

[20] Talabi, S.I., Owolabi, O.B., Adebisi, J.A., Yahaya, T. (2014). Effect of welding variables on mechanical properties of low carbon steel welded joint. Advances in Production Engineering & Management, 9(4): 181-186. http://doi.org/10.14743/apem2014.4.186

NOMENCLATURE

I	Welding current (A)
U	Arc voltage (V)

V	Welding (travel) speed (mm/s)
Fk	Tensile strength of weld joint (MPa)
Fv	Impact toughness (J)
R^2	Coefficient of determination
HV	Microhardness (Vickers)
HAZ	Heat-affected zone
S/N	Signal-to-noise ratio
DF	Degree of freedom
Adj-SS	Adjusted sum of squares
Adj-MS	Adjusted mean square
F-value	Fisher's ratio (variance ratio)
P-value	Probability value for significance testing

Subscripts

BM	Base Metal
WM	Weld Metal
FB	Fusion Boundary
opt	Optimal condition (e.g., Iopt = 125 A, Uopt = 20 V, Vopt = 3.5 mm/s)